Edgewise Bending Strain in Helical Coils With Geodesic Windings Based on Virial Theorem

Hiroaki Tsutsui, Shunji Tsuji-Iio, Shinichi Nomura, Tsuyoshi Yagai, Taketsune Nakamura, Hirotaka Chikaraishi, Nagato Yanagi, and Shinsaku Imagawa

***Abstract*—Distributions of edgewise bending strain in helical coils with the geodesic winding based on virial theorem are analyzed theoretically and numerically. A force-balanced coil (FBC) is a multipole helical coil combining toroidal field (TF) coils and a solenoid helically wound on a torus. The combination reduces the net electromagnetic force in the direction of the major radius by canceling out the centering force due to the TF coil current and the hoop force due to the solenoid current. The FBC concept was extended using the virial theorem, which shows the theoretical lower limit of stress in the coils and their supporting structure. High-field coils should accordingly have the same averaged principal stresses in all directions, which is named the virial-limit condition. Since FBC winding is modulated to reduce the tilting force, the winding is slightly similar to but different from the shortest geodesic trajectory and has no tensile load. To apply FBC to high-temperature superconducting tapes, the degradation of superconducting properties originating from edgewise bending strain is an important problem. Since the geodesic trajectory is a kind of a straight line on a curved surface and curves only to the normal direction of the surface, it is expected that the tape with geodesic trajectories has a small residual stress. In this paper, we analyze the effect of the winding modulations including the geodesic modulation for the optimization of residual stress in helical windings.**

***Index Terms*—Edgewise, geodesic, SMES, strain, torsion, virial theorem.**

I. Introduction

THE virial theorem provides a relation between the time average of the kinetic energy and that of the potential energy. A famous example is the relation between gravitational potential and kinetic energy in astrophysics [1]. In the field of superconducting magnetic energy storage (SMES), a relation between mass of the structure and stored energy is called the virial theorem [2], [3].

In the last decades, we had developed a SMES system with a force balanced coil (FBC) [4]–[6] which is a helical coil of toroidal field (TF) coils and a solenoidal coil. Their combination reduces the net electromagnetic force in major radius direction [4] by canceling the centering force of the TF coils and the hoop force of the solenoidal coil. Furthermore, we showed a configuration (named as the modulated winding) without overturning forces generated on the coils by giving poloidal dependence to pitch angle of helical winding [7]. Next we extended and generalized our studies with the virial theorem, and showed the theoretical lower limit of stress in coils. In addition, we conceptually designed a coil (virial-limit coil: VLC) with the minimum stress under the condition of a fixed magnetic energy [8]. It means that this coil enables us to make a SMES system with less amount of supporting structure, because the mass of the structure is proportional to the maximum stress. Following our theory, we designed and manufactured a coil-frame system [9], [10] in order to confirm our concept of minimum stress configuration. The coils, which are also designed following the modulated winding configuration, can generate strong magnetic field [11] even when the device size is small. However, it is difficult to make a larger device since the tension-free modulated winding configuration is mechanically unstable [12], and requires a great effort for windings.

Recently, we proposed a new modulated winding based on a geodesic which can be applied to windings under tension [13]. In order to apply FBC to high-temperature superconducting tapes, the degradation of superconducting properties originating from edgewise bending strain is an important problem [14]. Since a geodesic is a kind of straight line on a curved surface and curves only around the normal direction of the surface [15], it is expected that the tape with geodesic trajectories has a small residual stress. In this paper, we analyze the effect of the winding modulations including the geodesic modulation for the optimization of residual stress in helical windings.

In the next section, we explain a geodesic winding on a torus with an arbitrary cross section. The relation of the torsion and edgewise bending strain on the torus for the geodesic winding is also presented. In Section III, we investigate stress distribution numerically and show the effect of deformation of the torus, and summarize this work in Section IV.

II. Geodesic Winding on a Torus With Arbitrary Cross Section

The geodesic on a toroidal surface with a major radius R and a arbitrary cross section of a minor radius $\rho(\theta)$ is determined by a variation problem of

$$\delta S = 0 \tag{1}$$

$$S \equiv \oint ds \tag{2}$$

$$ds^2 = d\rho^2 + \rho^2 d\theta^2 + r^2 d\phi^2 \tag{3}$$

$$r = R + \rho\cos\theta \tag{4}$$

Manuscript received October 17, 2015; accepted February 18, 2016. Date of publication March 2, 2016; date of current version May 6, 2016.

H. Tsutsui and S. Tsuji-Iio are with the Research Laboratory for Nuclear Reactors, Tokyo Institute of Technology, Tokyo 152-8550, Japan (e-mail: htsutsui@nr.titech.ac.jp).

S. Nomura is with Meiji University, Tokyo 101-8301, Japan.

T. Yagai is with Sophia University, Tokyo 102-0094, Japan.

T. Nakamura is with Kyoto University, Kyoto 606-8501, Japan.

H. Chikaraishi, N. Yanagi, and S. Imagawa are with the National Institute for Fusion Science, Toki 509-5292, Japan.

Color versions of one or more of the figures in this paper are available online at http://ieeexplore.ieee.org.

Digital Object Identifier 10.1109/TASC.2016.2535779

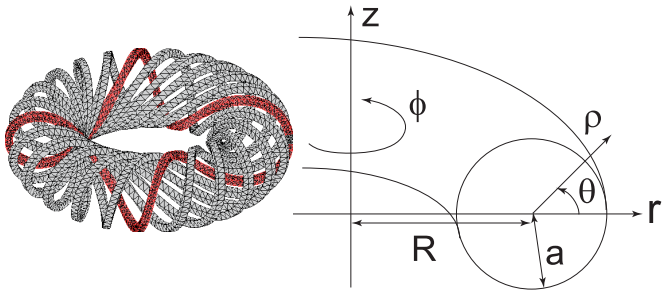

Fig. 1. Illustrations of a coil configuration and coordinate systems of cylindrical coordinate (r, z, ϕ) and semitoroidal coordinate (ρ, ϕ, θ), in which R and a are the major and minor radii of the coil, respectively.

where s is an arclength of a coil orbit (see Fig. 1). When we define the Lagrangian L,

$$L\left(\phi, \frac{d\phi}{d\theta}\right) \equiv \frac{ds}{d\theta} = \sqrt{\left(\frac{d\rho}{d\theta}\right)^2 + \rho^2 + r^2\left(\frac{d\phi}{d\theta}\right)^2} \quad (5)$$

$$S = \oint ds = \oint \frac{ds}{d\theta} d\theta = \oint L d\theta \quad (6)$$

the Euler-Lagrange equation is

$$\frac{d}{d\theta}\frac{\partial L}{\partial \dot{\phi}} = \frac{d}{d\theta}\left(\frac{r^2 \frac{d\phi}{d\theta}}{\sqrt{\left(\frac{d\rho}{d\theta}\right)^2 + \rho^2 + r^2\left(\frac{d\phi}{d\theta}\right)^2}}\right) = 0 \quad (7)$$

where $\dot{\phi} \equiv \frac{d\phi}{d\theta}$. The solution of (7) is

$$\frac{d\phi}{d\theta} = \frac{\rho}{r}\sqrt{\frac{1 + \left(\frac{d\log\rho}{d\theta}\right)^2}{\frac{r^2}{R^2\lambda^2} - 1}}. \quad (8)$$

Here λ is a non-dimensional integration constant related with the pitch number N, which is obtained from (8) as follows:

$$N = \oint \frac{d\theta}{d\phi} d\phi = 1/\int_0^{2\pi} \frac{d\phi}{d\theta} d\theta \quad (9)$$

and increases monotonously for $\lambda \to 0$ [13].

Using the Frenet frame [16], curvature κ and torsion τ of a trajectory $\boldsymbol{x}(s)$ is represented as follows:

$$\frac{d\boldsymbol{e}_1}{ds} = \kappa \boldsymbol{e}_2 \quad (10)$$

$$\frac{d\boldsymbol{e}_2}{ds} = -\kappa \boldsymbol{e}_1 + \tau \boldsymbol{e}_3 \quad (11)$$

$$\frac{d\boldsymbol{e}_3}{ds} = -\tau \boldsymbol{e}_2 \quad (12)$$

where $\boldsymbol{e}_i (i = 1, 2, 3)$ are basis vectors depicted in Fig. 2 and defined as

$$\boldsymbol{e}_1 = \frac{d\boldsymbol{x}}{ds} \quad (13)$$

$$\boldsymbol{e}_2 = \frac{\frac{d\boldsymbol{e}_1}{ds}}{\left|\frac{d\boldsymbol{e}_1}{ds}\right|} \quad (14)$$

$$\boldsymbol{e}_3 = \boldsymbol{e}_1 \times \boldsymbol{e}_2 \quad (15)$$

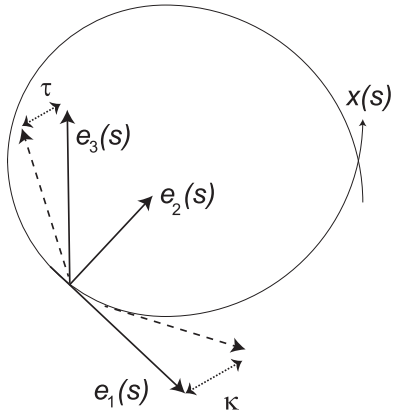

Fig. 2. Unit vectors $\boldsymbol{e}_i(s)(i = 1, 2, 3)$ in a Frenet frame, a curvature κ, and a torsion τ, where s is an arc length of a line.

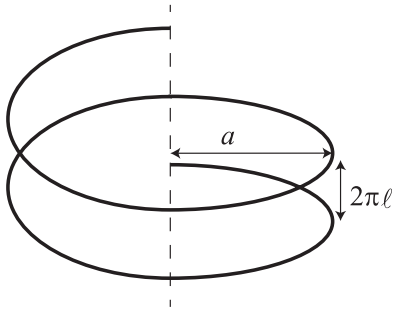

Fig. 3. Helix with radius a and pitch length ℓ.

where directions of $\boldsymbol{e}_i$ are orthogonal to each other, and called as tangential $(i = 1)$, principal normal $(i = 2)$ and binormal $(i = 3)$ directions, respectively. Although torsion τ is a function of a position, it has a uniform value,

$$\tau = \frac{\ell}{a^2 + \ell^2} \quad (16)$$

in the special case of a helix (Fig. 3) whose radius and pitch length are a and ℓ, respectively. If toroidal effects are neglected, the pitch length ℓ corresponds to R/N of the coil of a pitch number N on the torus with a major radius R. Then an averaged torsion of the torus is expected as follows:

$$\tau_{\text{ave}} = \frac{\frac{R}{N}}{a^2 + \left(\frac{R}{N}\right)^2} = \frac{1}{a}\frac{\frac{A}{N}}{1 + \left(\frac{A}{N}\right)^2} \leq \frac{1}{2a} \quad (17)$$

which has the maximum $1/2a$ in the case of $A = N$, where $A \equiv R/a$ is an aspect ratio of the torus.

Next, we consider a trajectory $\boldsymbol{x}_0(s)$ and another trajectory $\boldsymbol{x}_h(s)$ which is h away from the trajectory $\boldsymbol{x}_0(s)$ to binormal direction $\boldsymbol{e}_3$,

$$\boldsymbol{x}_h(s) = \boldsymbol{x}_0(s) + h\boldsymbol{e}_3 \quad (18)$$

where s is the arclength of the trajectory $\boldsymbol{x}_0$. Differentiating (18) by s, the following equation is obtained,

$$\frac{d\boldsymbol{x}_h}{ds} = \frac{d\boldsymbol{x}_0}{ds} + h\frac{d\boldsymbol{e}_3}{ds} = \boldsymbol{e}_1 - h\tau\boldsymbol{e}_2 \quad (19)$$

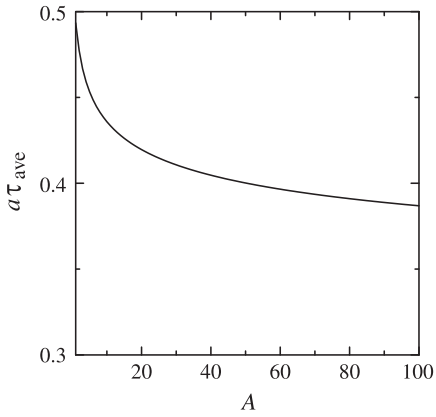

Fig. 4. Averaged torsion $a\tau_{\rm ave}$ (17) normalized by a minor radius a as a function of aspect ratio $A = R/a$ under the virial-limit condition (22).

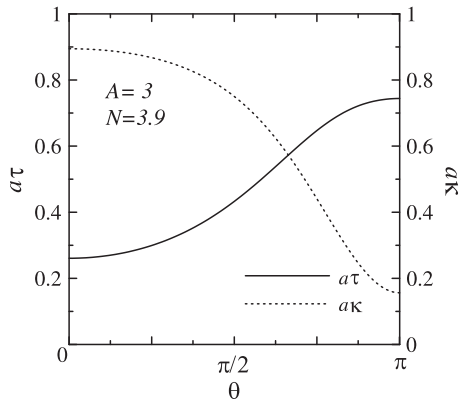

Fig. 5. Longitudinal distribution of normalized torsion $a\tau$ (solid line) and curvature $a\kappa$ (dotted line) of a geodesic trajectory on a circular cross section with $A = 3$ and $N = 3.9$.

using (12) and (13). Then the following relation holds,

$$ds_h^2 \equiv |d\boldsymbol{x}_h|^2 = (1 + h^2\tau^2)ds^2 \tag{20}$$

and strain ϵ satisfies the next relation:

$$\epsilon = \frac{ds_h - ds}{ds} = \sqrt{1 + h^2\tau^2} - 1 \simeq \frac{1}{2}(h\tau)^2. \tag{21}$$

Since the principal normal direction of geodesic trajectories coincides with the normal direction of the toroidal surface [16], the strain (21) is an edgewise bending strain in a tape-shaped conductor. Then the edgewise bending strain of high-temperature superconducting tapes is proportional to the square of torsion, and the reduction of residual stress requires the reduction of torsion.

III. Numerical Results

As was mentioned in the previous section, a square of torsion of geodesic trajectories is proportional to the residual strain of coils. In this section, we numerically evaluate the torsion distribution. In the case of the pitch number N or for an aspect ratio $A = R/a$ much greater than unity, toroidal effects are negligible, and (17) is applied. Since the virial-limit condition of the torus is [8],

$$N^2 = \frac{2}{3}A^2 \log 8A \tag{22}$$

the combination of these equations (17) and (22) gives a relation of averaged torsion $\tau_{\rm ave}$ and aspect ratio A as shown in Fig. 4. Therefore, large aspect ratio is desirable to reduce the edgewise bending strain because $\tau_{\rm ave}$ is a monotonic decreasing function of A.

By use of Frenet frame (10)–(12), a curvature κ and torsion τ of trajectory $\boldsymbol{x}(t)$ are evaluated as follows [16]:

$$\kappa(t) = \sqrt{\frac{(\dot{\boldsymbol{x}},\dot{\boldsymbol{x}})(\ddot{\boldsymbol{x}},\ddot{\boldsymbol{x}}) - (\dot{\boldsymbol{x}},\ddot{\boldsymbol{x}})^2}{(\dot{\boldsymbol{x}},\dot{\boldsymbol{x}})^3}} \tag{23}$$

$$\tau(t) = \frac{\det(\dot{\boldsymbol{x}},\ddot{\boldsymbol{x}},\dddot{\boldsymbol{x}})}{(\dot{\boldsymbol{x}},\dot{\boldsymbol{x}})(\ddot{\boldsymbol{x}},\ddot{\boldsymbol{x}}) - (\dot{\boldsymbol{x}},\ddot{\boldsymbol{x}})^2} \tag{24}$$

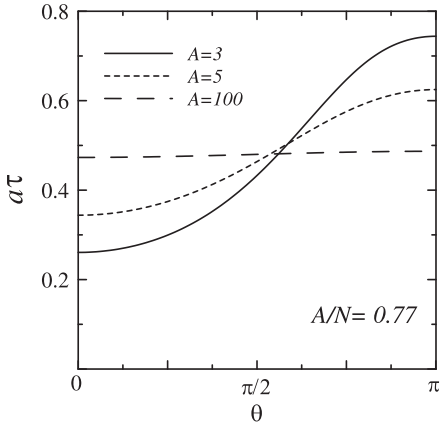

Fig. 6. Longitudinal distributions of normalized torsions $a\tau$ for several aspect rations of $A = 3$, 5, 100 under the condition of $A/N = 0.77$. Here, N is a pitch number of windings, and A/N corresponds to the pitch length on a helix.

where a dot means a derivation by an arbitrary parameter t which uniquely determines the location on the trajectory, and is chosen as θ in this work whereas θ is also a coordinate variable. These κ and τ can be computed only by the solution (8) of Euler-Lagrange equation for geodesic windings. Fig. 5 shows a longitudinal distributions of torsion τ and curvature κ of a trajectory on a torus with $A = 3$ and $N = 3.9$. Non-uniformity of τ by toroidal effects are represented, and the torsion has a maximum at the inside ($\theta = \pi$) on the torus.

Next, we investigate the dependence on toroidal effects. Fig. 6 shows longitudinal distribution of torsions τ for some aspect ratios under the condition of $A/N = 0.77$. Variations of τ decrease according as A increases, and it converges to $\tau_{\rm ave} = 0.48/a$ for $A = 100$. The dependence on the pitch number N is also investigated in Fig. 7. Even if aspect ratio A is small, a trajectory with a large pitch number N is not sensitive to toroidal effects. As is shown in Fig. 7, the values of torsion decreases with N, and finally becomes zero. In the limit of $N \to \infty$, the trajectory becomes a circle of radius a, which is a curvature radius, without torsion.

Finally, we investigate the effects of deformation of a cross section of the toroidal winding frame. In the former calculations, a circular cross section was used. Here, we introduce

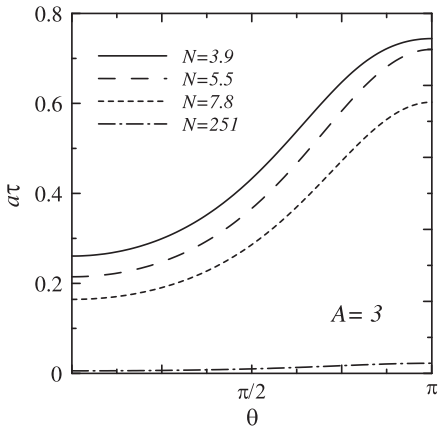

Fig. 7. Longitudinal distributions of normalized torsions $a\tau$ for several pitch numbers of $N = 3.9$ to 251 under the condition of $A = R/a = 3$.

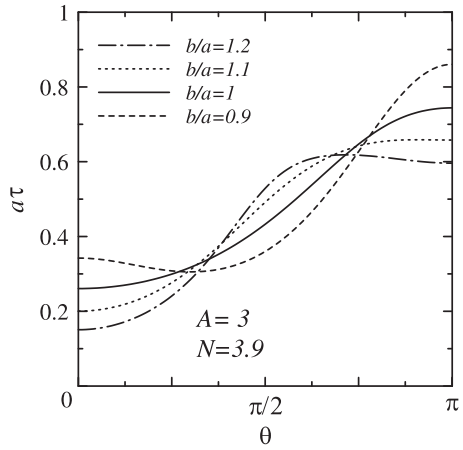

Fig. 8. Longitudinal distributions of normalized torsions in the coil of $N = 3.9$ on the torus with $A = 3$, whose ellipticity is changed from $b/a = 0.9$ to 1.2.

ellipticity b/a, where a and b are radii of a cross section of a torus in horizontal and vertical directions, respectively. When the cross section is flattened $(a > b)$, the maximum of τ at $\theta = \pi$ increases, while the distribution of τ around $\theta = \pi$ becomes flattened and the maximum of τ decreases according to the increase of b/a as shown in Fig. 8. When b/a exceeds 1.2 in the case of $A = 3$ and $N = 3.9$, the direction of curvature vector is reversed, and the coil with a tension is detached from the torus [13]. Therefore, the maximum of torsion in the geodesic coil of $N = 3.9$ on the torus with $A = 3$ has the smallest value $\tau \simeq 0.6/a$ which is similar to $\tau_{\rm ave}$ for $b/a = 1.2$. As was shown in this work, $\tau \sim \tau_{\rm ave} \sim 1/2a$. Therefore, the edgewise strain ϵ is

$$\epsilon = \frac{1}{2}(h\tau)^2 \sim \frac{1}{8}\left(\frac{h}{a}\right)^2 \tag{25}$$

which is sufficiently small to degrade the superconducting properties for $h/a < 0.1$ [17].

IV. Conclusion

By use of Frenet frame, we derived the relation of edgewise bending strain ϵ and a torsion τ in the geodesic winding coils in which ϵ is proportional to square of τh, where h is a width of a tape-shaped conductor. Next, we analytically derived the orbit equation of the geodesic winding on the axisymmetric torus with an arbitrary cross section. Using this orbit equation, longitudinal distributions of torsion were evaluated for geodesic winding orbits on various tori. We showed that longitudinal distribution of torsion in a coil on the torus with a cross section slightly elongated vertically is flattened around its maximum point. Although the distribution of strain depends on the shape of the cross section, the edgewise bending strain ϵ is the same in the order of magnitude as $\frac{1}{8}(h/a)^2$.

References

[1] G. W. Collins, *The Virial Theorem in Stellar Astrophysics*. Tucson, AZ, USA: Pachart Publishing House/NASA Astrophysics Data System, 1978.
[2] C. L. Longmire, *Elementary Plasma Physics*. New York, NY, USA: Wiley, 1963, pp. 68–73.
[3] F. C. Moon, "Buckling of a superconducting coil nested in a three-coil toroidal segment," *J. Appl. Phys.*, vol. 53, no. 12, pp. 9112–9121, Mar. 1982.
[4] Y. Miura, M. Sakota, and R. Shimada, "Force-free coil principle applied to helical winding," *IEEE Trans. Magn.*, vol. 30, no. 4, pp. 2573–2576, Jul. 1994.
[5] Y. Sato *et al.*, "Experiment of the force-balanced coil for superconducting magnetic energy storage," in *Proc. 15th Int. Conf. Magnet Technology*, pp. 402–409, Beijing, China, Oct. 20–24, 1997.
[6] S. Nomura *et al.*, "Design considerations for force-balanced coil applied to SMES," *IEEE Trans. Appl. Supercond.*, vol. 11, no. 1, pp. 1920–1923, Mar. 2001.
[7] J. Kondoh *et al.*, "Application of a force-balanced coil to a tokamak device," *IEEJ Trans. Power Energy*, vol. 118-B, no. 2, pp. 191–198, 1998.
[8] H. Tsutsui, S. Nomura, and R. Shimada, "Optimization of SMES coil by using virial theorem," *IEEE Trans. Appl. Supercond.*, vol. 12, no. 1, pp. 800–803, Mar. 2002.
[9] S. Nomura *et al.*, "Demonstration of the stress minimized force-balanced coil concept for SMES," *IEEE Trans. Appl. Supercond.*, vol. 13, no. 2, pp. 1852–1855, Jun. 2003.
[10] S. Nomura *et al.*, "Experimental results of a 7-T force-balanced helical coil for large-scale SMES," *IEEE Trans. Appl. Supercond.*, vol. 18, no. 2, pp. 701–704, Jun. 2008.
[11] S. Nomura *et al.*, "Quench properties of a 7-T force-balanced helical coil for large-scale SMES," *IEEE Trans. Appl. Supercond.*, vol. 19, no. 3, pp. 2004–2007, Jun. 2009.
[12] T. Habuchi, H. Tsutsui, S. Tsuji-Iio, and R. Shimada, "Force balance and stability of toroidally helical coil with circular cross-section," *J. Plasma Fusion Res.*, vol. 6, 2011, Art. no. 2405150.
[13] H. Tsutsui *et al.*, "Analysis of stress distribution in helical coils with geodesic windings based on virial theorem," *IEEE Trans. Appl. Supercond.*, vol. 22, no. 3, Jun. 2012, Art. no. 4705604.
[14] P. Vase, R. Flukiger, M. Leghissa, and B. Glowacki, "Current status of high-T_c wire," *Supercond. Sci. Technol.*, vol. 13, no. 7, pp. R71–R84, Jul. 2000.
[15] G. Sapiro, "Geodesic curves and minimal surfaces," in *Geometric Partial Differential Equations and Image Analysis*. Cambridge, U.K.: Cambridge Univ. Press, 2006.
[16] J. J. Stoker, "Space Curves," in *Differential Geometry*. Hoboken, NJ, USA: Wiley, 1988.
[17] T. Yagai *et al.*, "Strain distribution of complex-bending YBCO tape in force-balanced coil applied to SMES," presented at the 24th Int. Conf. Magnet Technology, Seoul, South Korea, Oct. 18–23, 2015, Paper 1PoBG07.